Electronic Supplementary Material (ESI) for RSC Advances.

Supplementary text

An effective utilization of MXene and its effect on electromagnetic interference shielding: flexible, free standing and thermally conductive composite from MXene-PAT-Poly(p-aminophenol)-polyaniline co-polymer.

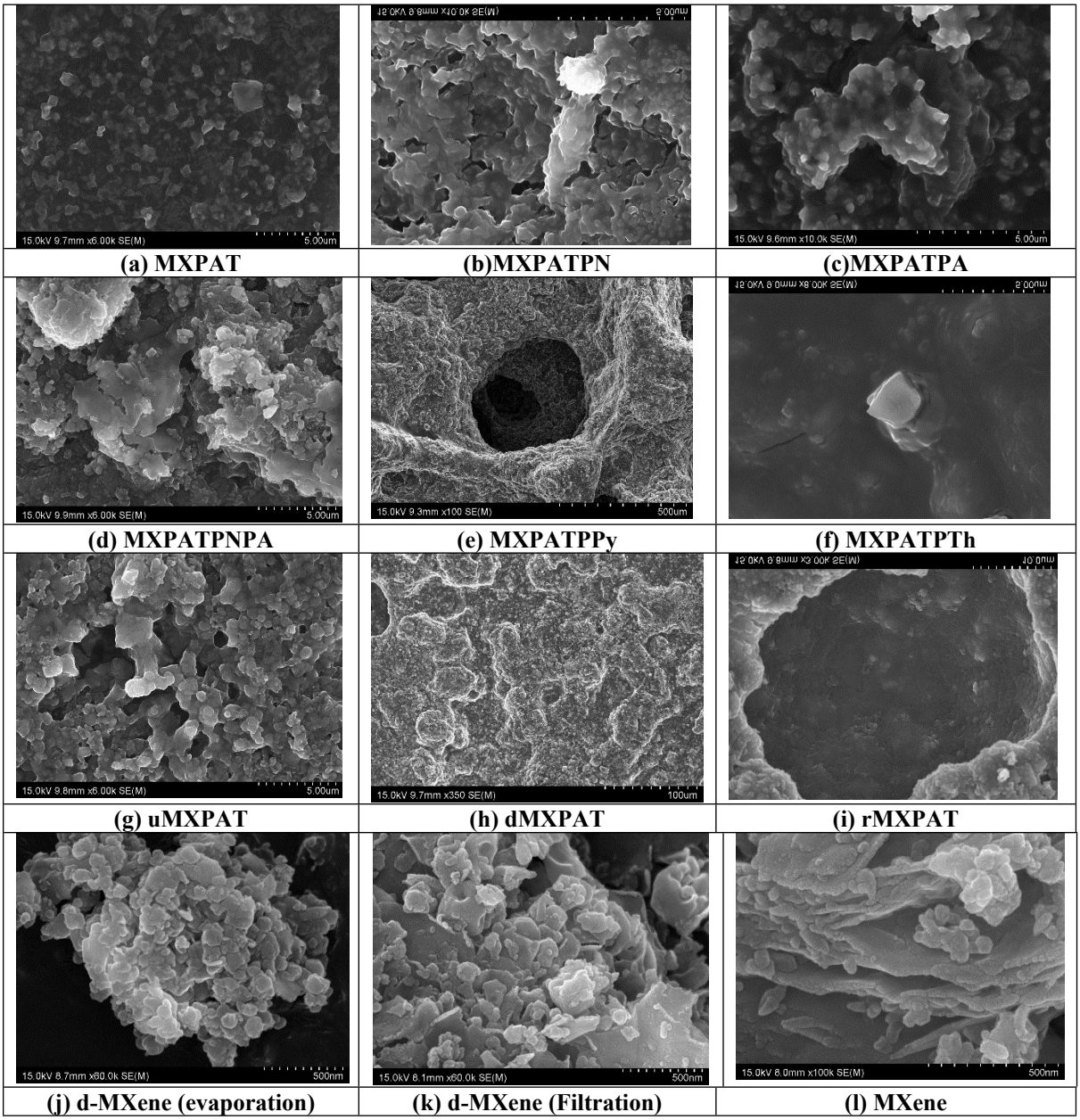

Figure S1. The topology of the composite and MXene under the scanning electron microscope.

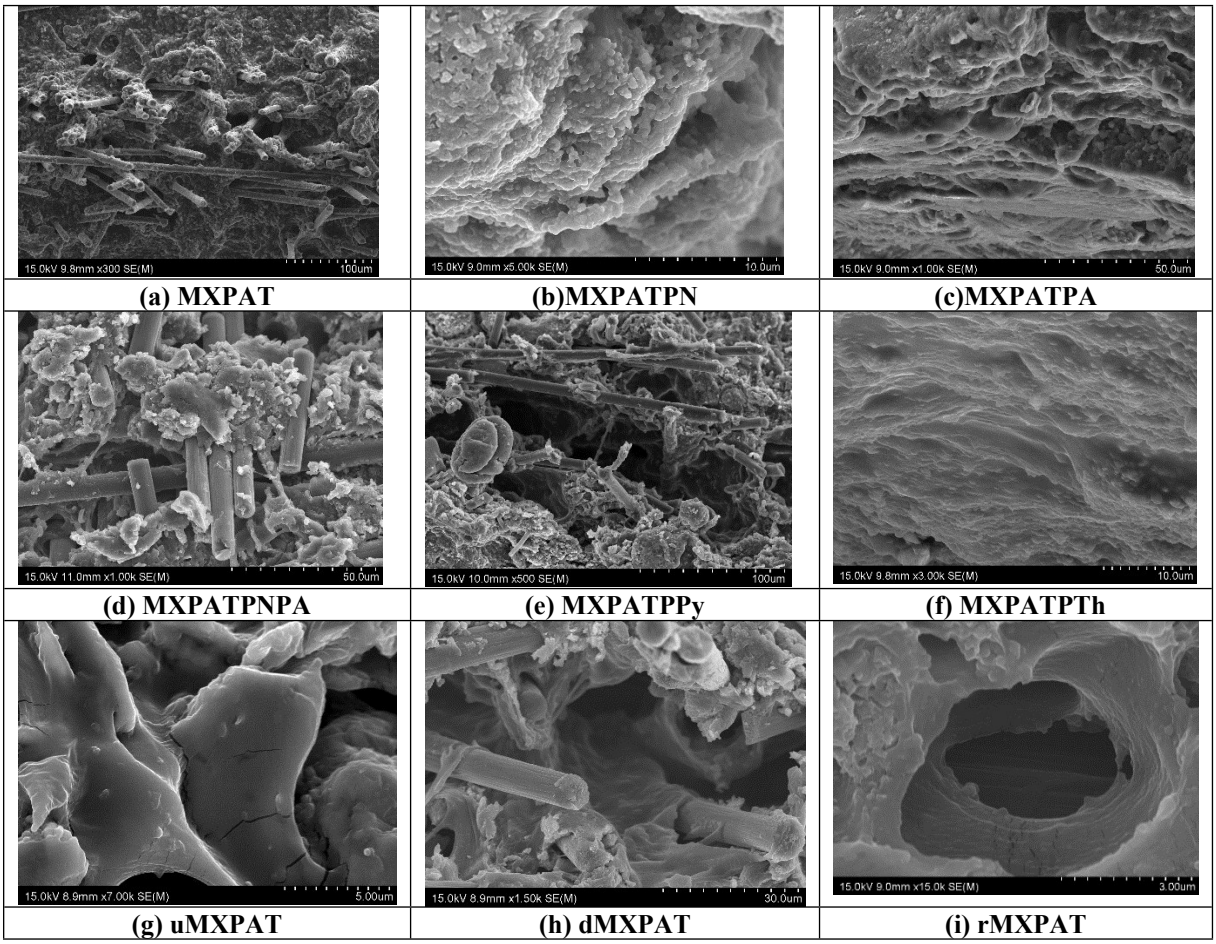

Figure S2. The cross-section of the composite under the scanning electron microscope.

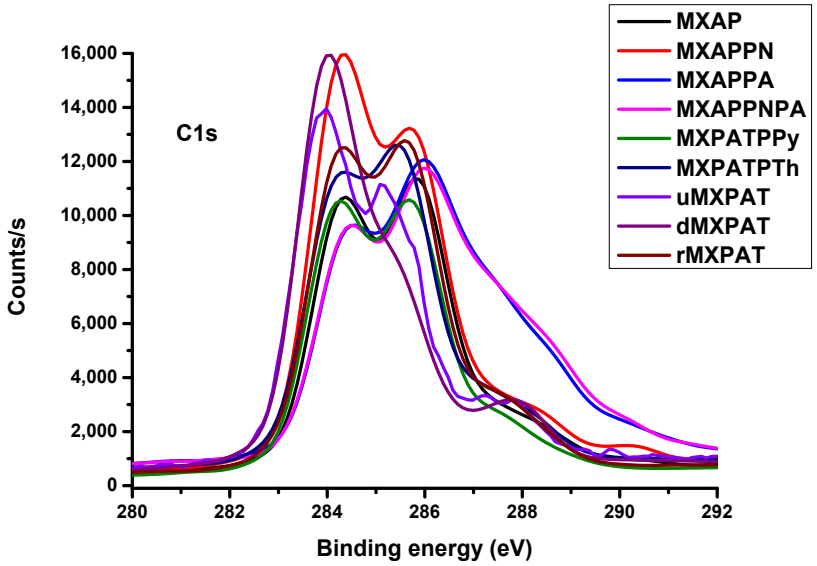

Figure S3. XPS O1s Overlapping curve of composites

Table S1. Elemental percentage of composites from XPS

Nos	Composites	C1s %	Ti2p %	O1s %	F1s %	N1s %	S2p %

1	MXPAT	65.51	0.49	32.4	1.6	-	-
2	MXPATPN	67.24	0.68	27.6	2.53	1.94	-
3	PXPATPA	62.75	0.57	32.07	1.79	2.83	-
4	MXPATPNPA	62.94	0.55	31.84	1.54	3.14	-
5	MXPATPPy	62.35	1.04	32.78	1.76	2.07	-
6	MXPATPTh	62.43	0.41	34.09	0.74	-	2.32
7	uMXPAT	65.27	0.68	31.18	2.88	-	-
8	dMXPAt	70.5	0.71	27.38	1.41	-	-
9	rMXPAT	62.81	0.33	34.74	2.11	-	-

Table S2. Peak position of elements in composites from XPS

Elements	MXPAT	MXPATPN	MXPATPA	MXPATPNPA	MXPATPPy	MXPATPTh	uMXPAT	dMXPAT	rMXPAT
C1S	285.66	284.49	285.78	285.84458.31	285.1	285.14	284.12	284.05	284.66
Ti2p	474.98	458.55	458.87	532.49	448.18	457.24	457.9	457.99	460.91
O1s	544.98	532.12	532.5	687.49	525.18	531.78	531.41	531.31	531.97
F1s	697.98	687.36	687.51	401.44	678.18	683.72	684.72	684.89	685.18
N1s	-	399.48	401.49	-	399.5	-	-	-	-
S2p	-	-	-	-	-	167.75	-	-	-

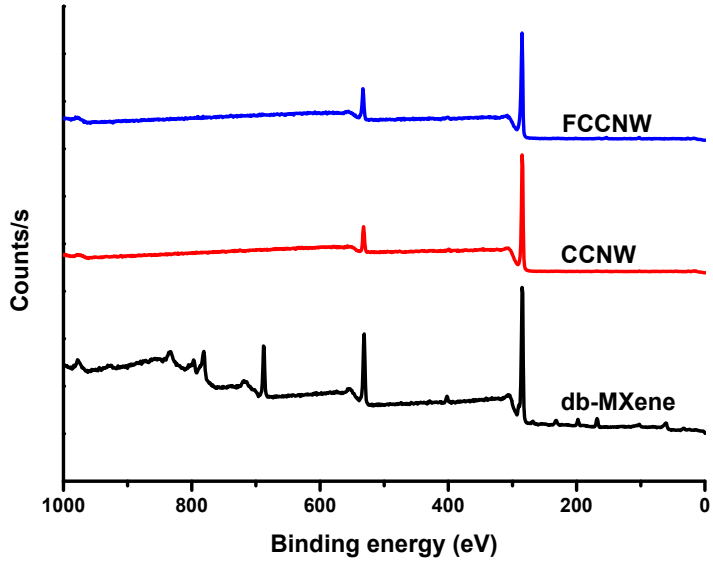

Figure S4. XPS of FCCNW, CCNW and db-MXene

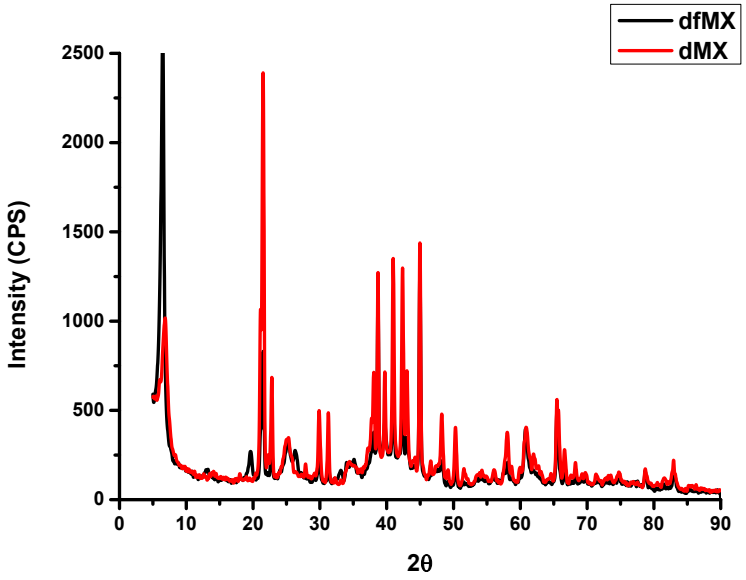
dfMX
dMX
Intensity (CPS)
2θ
0
500
1000
1500
2000
2500
0
10
20
30
40
50
60
70
80
90

(a)

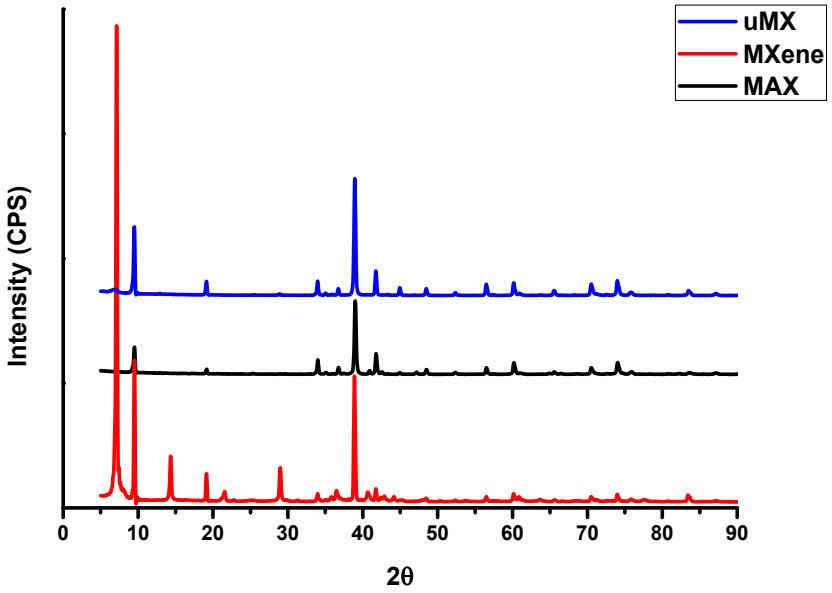
uMX
MXene
MAX
Intensity (CPS)
2θ
0
10
20
30
40
50
60
70
80
90

(b)

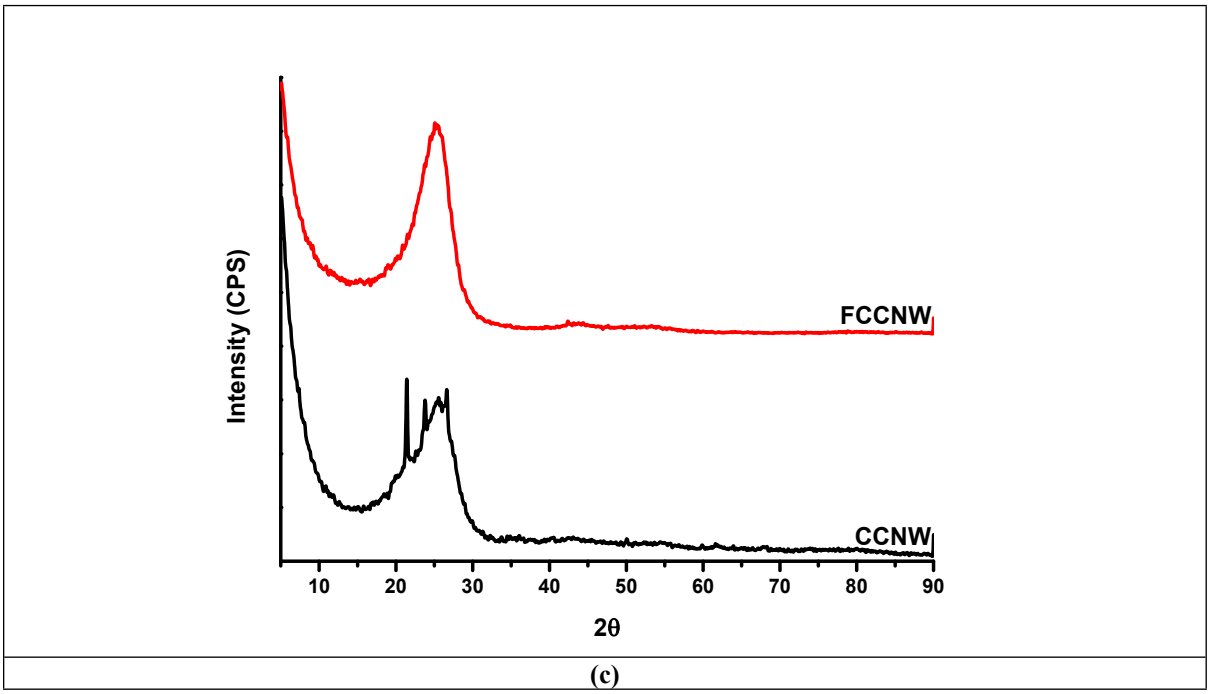

(c)

Figure S5. XRD of df-MXene, d-MXene, u-MXene, MAX phase, CCNW and FCCNW.

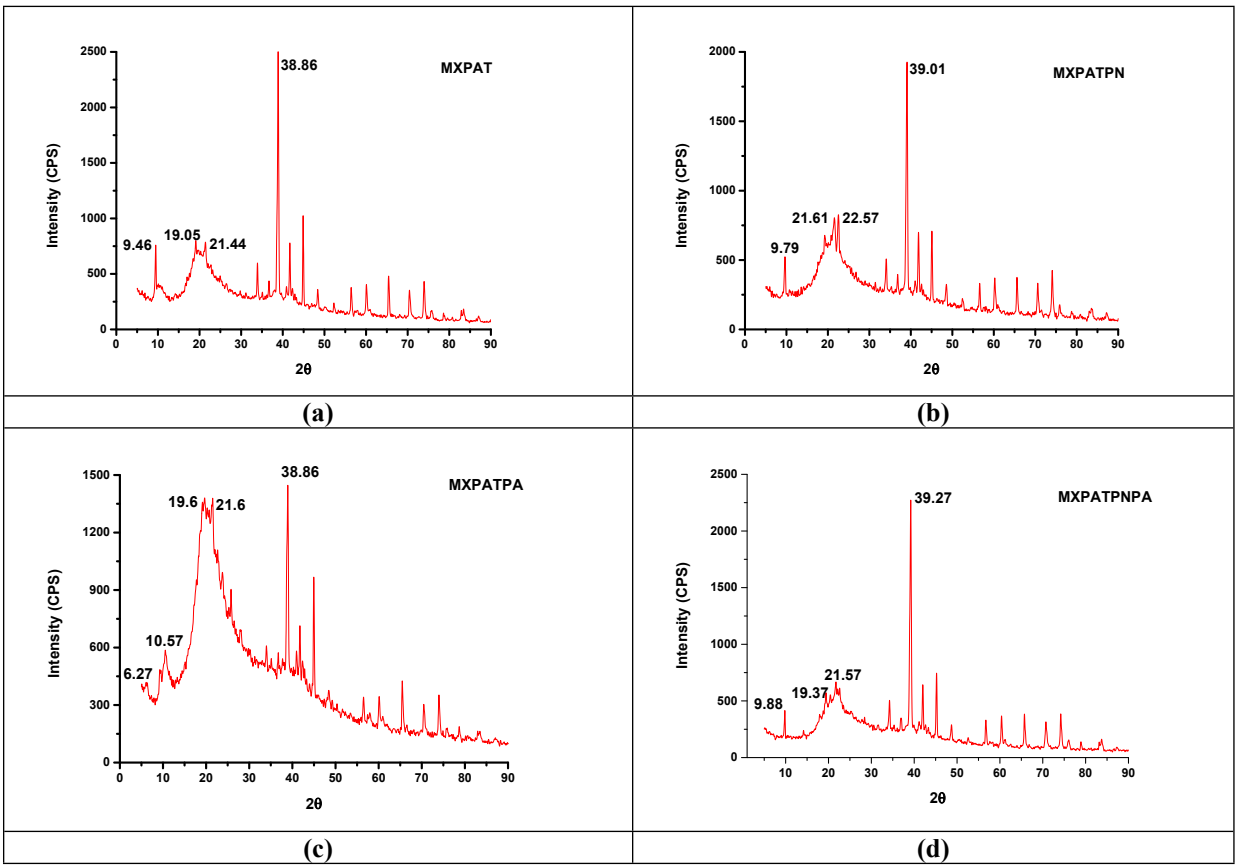

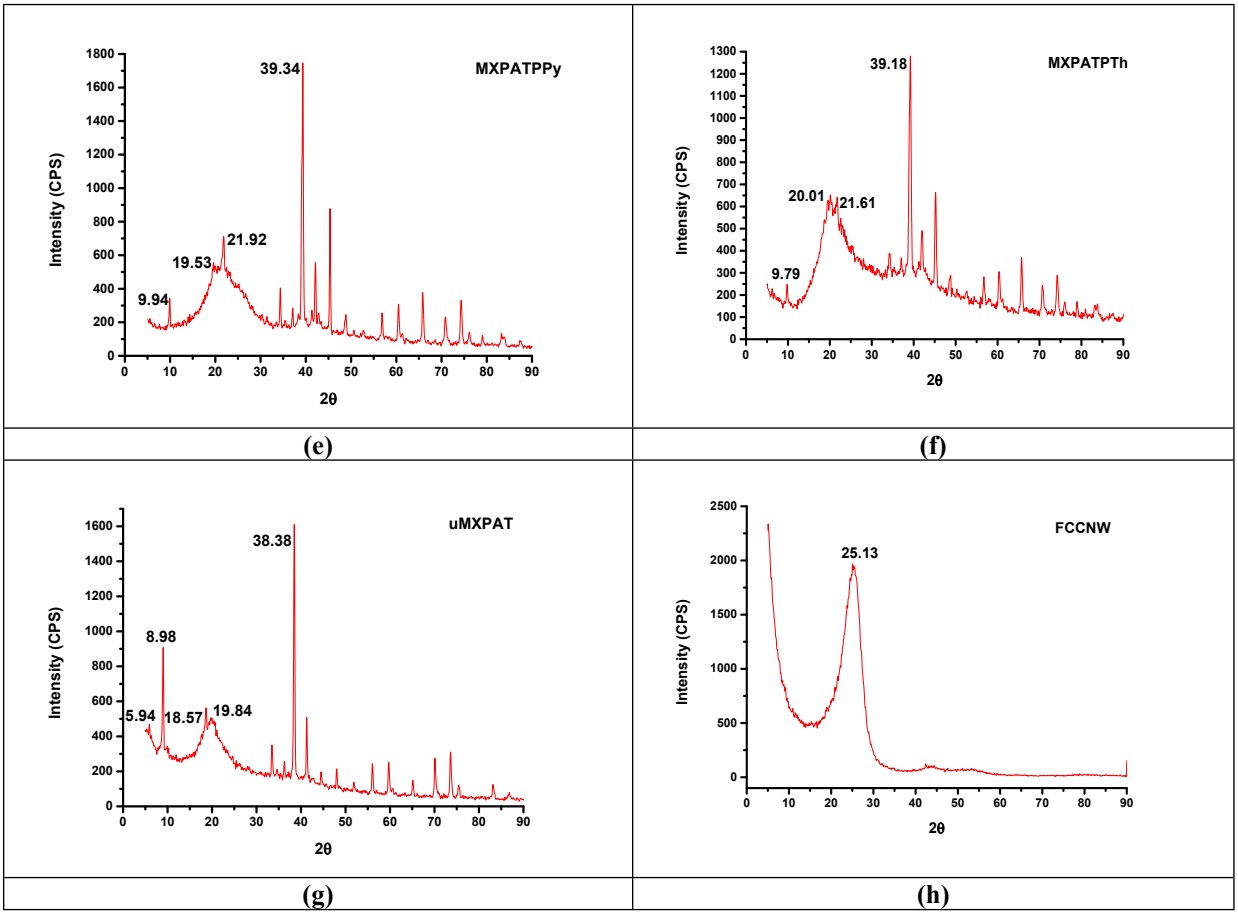

Figure S6. XRD of composites

Table S3. XRD peaks of composites

Composites	Peak positions (2θ angle)		
MXPAT	9.46	19.05, 21.44	33.92, 36.78, 38.78, 38.86, 41.74, 44.93, 48.45, 50.35, 52.28, 56.43, 60.10, 65.39, 70.33, 74.00, 75.77, 78.64, 82.79, 83.44, 87.11
MXPATPN	9.79	18.4, 19.36, 21.61, 22.57, 25.9	34.1, 36.93, 39.01, 41.89, 45.08, 48.61, 52.45, 56.60, 60.28, 65.54, 70.66, 74.18, 75.77, 78.81, 80.88, 83.60, 87.27
MXPATPA	6.27, 10.57	19.6, 21.6, 23.9, 25.8	33.92, 35.03, 36.63, 38.86, 40.93, 41.74, 44.93, 48.45, 56.60, 57.87, 60.10, 65.54, 70.50, 74.00, 75.77, 78.64, 83.27, 87.12
MXPATPNPA	9.88	19.37, 20.47, 21.57, 22.67	28.53, 31.69, 34.22, 35.32, 36.89, 39.27, 41.95, 45.11, 48.74, 52.69, 56.89, 60.43, 65.82, 70.87, 74.18, 76.08, 78.93, 83.82, 87.45
MXPATPPy	9.94	19.53, 21.92, 25.3, 25.9	34.39, 35.51, 37.11, 39.34, 41.26, 42.22, 43.01, 45.41, 48.93, 50.68, 52.60, 56.91, 60.58, 65.87, 68.74, 70.97, 74.33, 76.25, 78.96, 83.27, 87.59
MXPATPTh	9.79	20.01, 21.61	34.22, 35.33, 36.39, 39.18, 42.05, 45.26, 48.76, 50.35, 52.60, 54.53, 56.76, 60.43, 65.70, 70.66, 74.33, 76.01, 78.96, 81.04, 83.27, 83.27, 83.92, 87.60
uMXPAT	5.94, 8.98	18.57, 19.84	33.44, 34.71, 36.15, 38.38, 41.26, 44.45, 48.12, 51.97, 56.12, 59.79, 65.22, 70.18, 73.52, 75.29, 83.12, 86.94

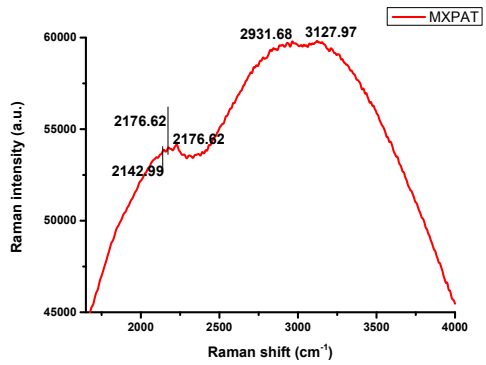
MXPAT
2931.68
3127.97
2176.62
2176.62
2142.99
Raman intensity (a.u.)
Raman shift (cm-1)

(a)

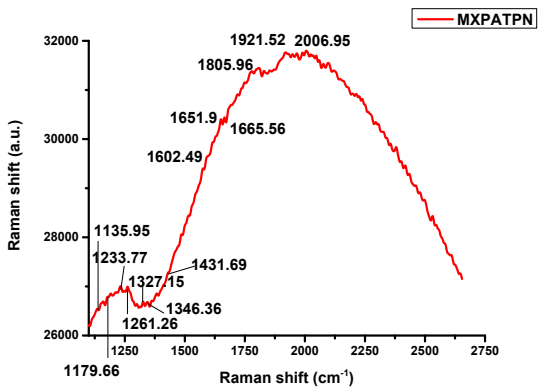
MXPATPN
1921.52
2006.95
1805.96
1651.9
1665.56
1602.49
1135.95
1233.77
1431.69
1327.15
1346.36
1261.26
1179.66
Raman shift (a.u.)
Raman shift (cm-1)

(b)

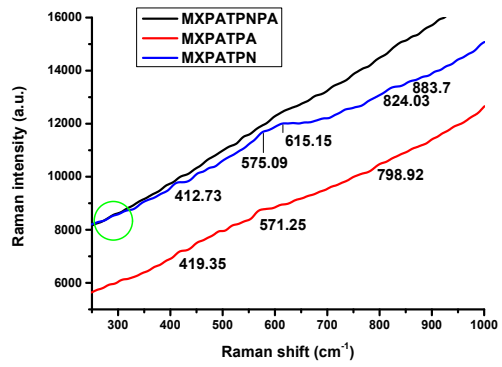
MXPATPNPA
MXPATPA
MXPATPN
883.7
824.03
615.15
575.09
798.92
412.73
571.25
419.35
Raman intensity (a.u.)
Raman shift (cm-1)

(c)

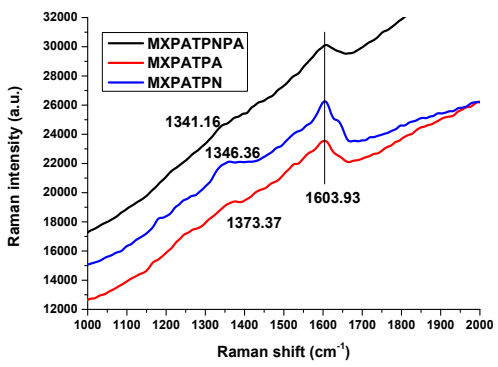
MXPATPNPA
MXPATPA
MXPATPN
1341.16
1346.36
1603.93
1373.37
Raman intensity (a.u.)
Raman shift (cm-1)

(d)

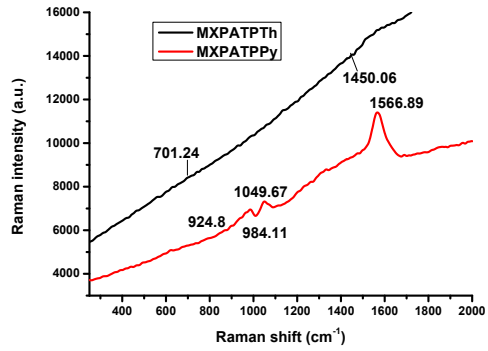
MXPATPTh
MXPATPPy
1450.06
1566.89
701.24
1049.67
924.8
984.11
Raman intensity (a.u.)
Raman shift (cm-1)

(e)

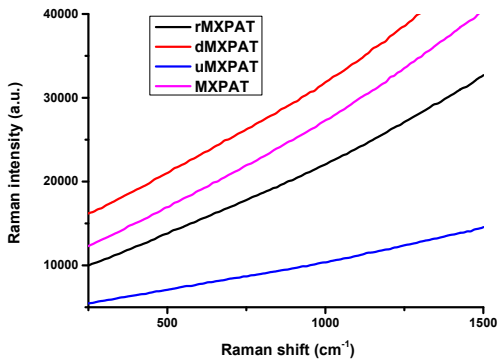
rMXPAT
dMXPAT
uMXPAT
MXPAT
Raman intensity (a.u.)
Raman shift (cm-1)

(f)


rMXPAT
dMXPAT
uMXPAT
MXPAT
Smoothed Y4
Raman shift

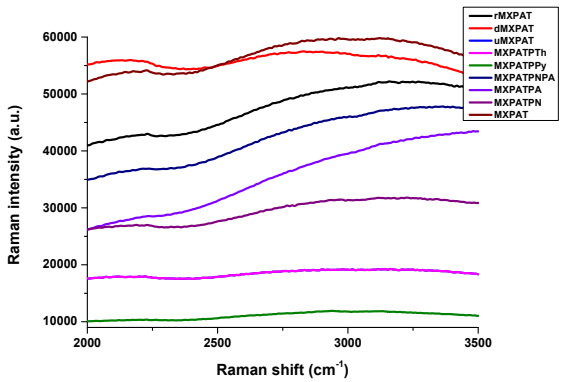
rMXPAT
dMXPAT
uMXPAT
MXPATPTh
MXPATPPy
MXPATPNPA
MXPATPA
MXPATPN
MXPAT
Raman intensity (a.u.)
Raman shift (cm-1)

(h)	(i)

Figure S7. Raman spectra comparison of composite in different range.

Table S4. Peak position of Raman shift

Composites	Peak positions (cm^{-1})
MXPAT	2176.62, 2931.68, 2230.85, 3127.97
MXPATPN	412.73, 824.03, 883.7, 1135.95, 1179.66, 1327.15, 1346.36, 1431.69, 1602.49, 1651.99, 1665.56, 1805.96, 1921.52, 2006.95, 2183.51, 2774.51, 2969.56, 3121.13, 3223.35
MXPATPA	1373.37, 1597.79, 2217.58, 3125.83
MXPATPNPA	1608.20, 2215.77, 3009.19, 3350.14
MXPATPPY	984.11, 1049.67, 1566.89, 2221.85, 2937.75, 3129.80
MXPATPTh	2117.92, 2224.20, 2903.55, 3169.52
uMXPAT	2109.29, 2072.44, 2219.35, 2905.28, 3162.74
dMXPAT	1761.03, 2144.29, 2827.47, 3117.97
rMXPAT	2238.50, 3163.90

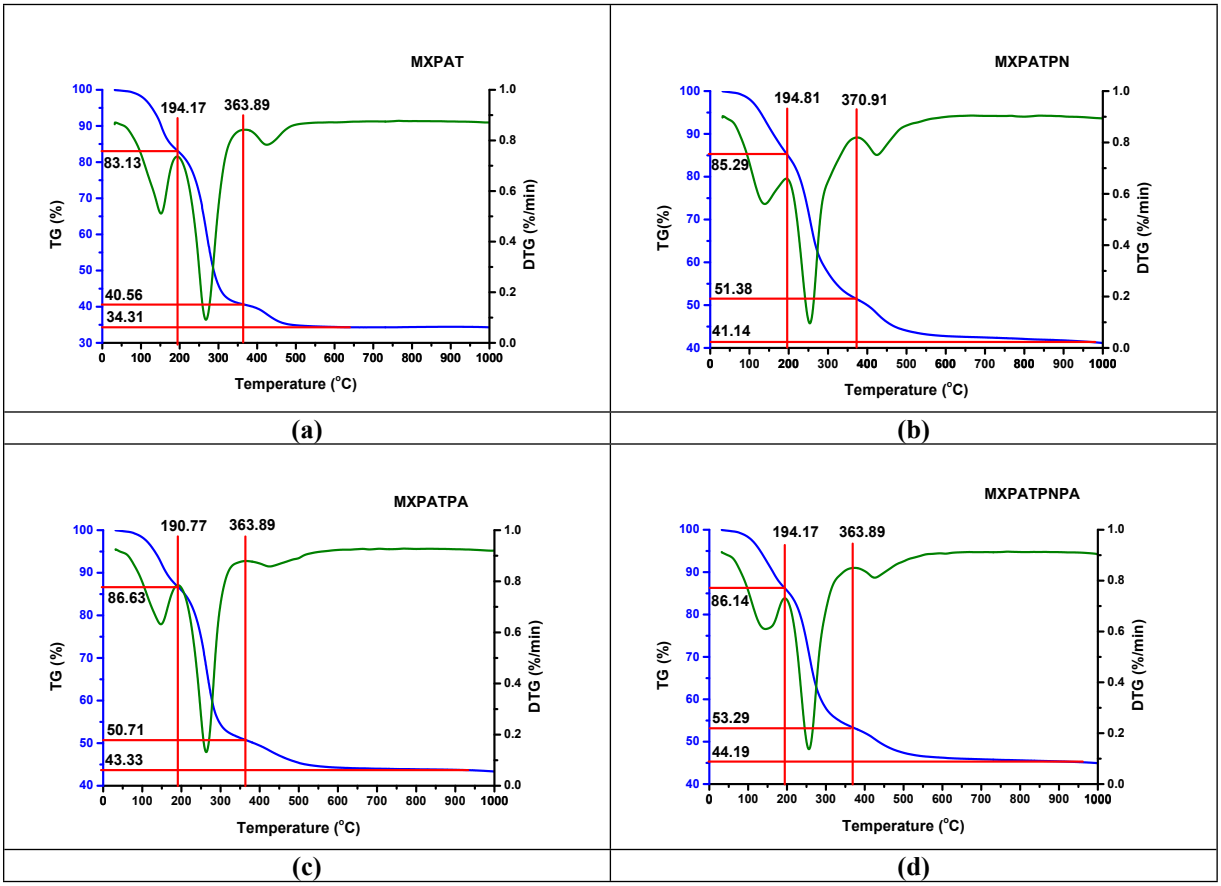

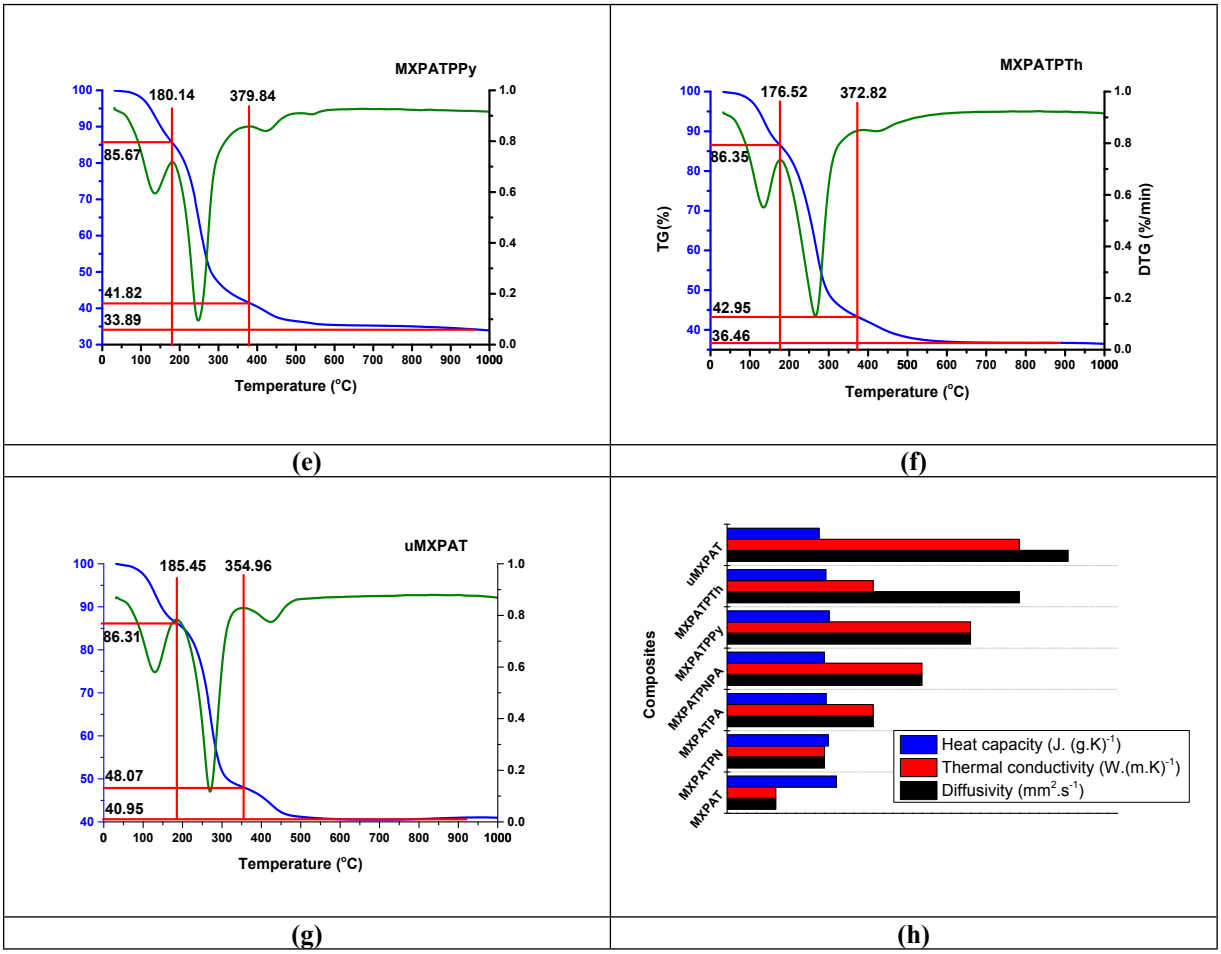

Figure S8. (a-g) TGA and DTG analysis of composites (h) Thermal diffusivity, thermal conductivity and Heat capacity of the composites.

Table S5. Thermogravimetric analysis (TG) of the composites

Composites	Temperature	Total weight loss (%)
MXPAT	30-194.17 194.17-363.89 363.89-1000	16.81 59.44 65.69
MXPATPN	30-194.81 194.81-370.91 370.91-1000	14.71 48.62 58.86
MXPATPA	30-190.77 190.77-363.89 363.89-1000	13.37 49.29 56.67
MXPATPNPA	30-194.17 194.17-363.89 363.89-1000	13.86 46.71 55.09
MXPATPPy	30-180.14 180.14-379.84 379.84-1000	14.33 58.18 66.11
MXPATPTh	30-176.52 176.52-372.82 372.82-1000	13.65 57.05 63.54
uMXPAT	30-185.45 185.45-354.96 354.96-1000	13.69 51.93 59.05

Table S6. Derivative Thermogravimetry (DTG) analysis

Composites	Endothermic peaks	Exothermic peaks
MXPAT	151.85, 266.69, 424.08	194.17, 363.89
MXPATPN	139.52, 254.36, 424.08	194.81, 370.91
MXPATPA	146.53, 263.08, 424.08	190.77, 363.89
MXPATPNPA	146.53, 256.06, 424.08	194.17, 363.89
MXPATPPy	135.90, 247.34, 424.08	180.14, 379.84
MXPATPTh	134.20, 266.70, 424.08	176.52, 372.82
uMXPAT	128.88, 270.31, 424.08	185.45, 354.96

Table S7. SE of fabricated composites

SE(dB)	MXPAT	MXPATPN	MXPATPA	MXPATPNPA	MXPATPPy	MXPATPTh	uMXPAT	dMXPAT	rMXPAT
MAX	41.31	39.33	45.18	44.08	41.31	42.99	39.69	43.74	44.31
MIN	38.55	37.83	39.00	37.87	39.65	40.25	36.04	41.54	39.94
Aveage	39.29	38.24	40.48	40.96	40.00	41.44	37.25	42.40	42.15
SSE ($dB.g^{-1}.cm^3$)	29.95	27.99	33.26	31.98	40.49	33.10	28.85	-	-
SSE/t ($dB.g^{-1}.cm^2$)	575.96	321.72	236.45	399.75	253.06	359.78	721.25	-	-
SE/t ($dB.m\ m^{-1}$)	1.463	1.393	1.6	1.561	1.463	1.522	1.406	1.549	1.569

Table S8. SE_A of fabricated composites

SE_A (dB)	MXPAT	MXPATPN	MXPATPA	MXPATPNPA	MXPATPPy	MXPATPTh	uMXPAT	dMXPAT	rMXPAT
Max	30.58	30.44	34.85	36.56	37.57	34.87	29.99	34.48	34.09
Min	28.25	29.37	29.81	29.46	36.46	30.62	26.24	32.91	29.72
Average	29.17	29.83	31.13	33.28	36.77	32.99	27.55	33.50	32.02

Table S9. SE_R of fabricated composites

SE_R (dB)	MXPAT	MXPATPN	MXPATPA	MXPATPNPA	MXPATPPy	MXPATPTh	uMXPAT	dMXPAT	rMXPAT
MAX	11.44	9.84	10.34	9.09	4.71	9.77	10.11	9.77	11.43
Min	9.27	7.40	8.41	7.37	2.27	7.87	9.18	8.49	9.47
Average	10.12	8.42	9.36	7.69	3.24	8.45	9.69	8.91	10.13

Table S10. The bandwidth comparison at about 99.99% shielding efficiency.

Composites	EMI SE at 99.99% efficiency (dB)	Maximum point (dB)	Bandwidth (GHz)	Range (GHz)
MXPAT	39.88	41.31	8.82-12.4	3.58
dMXPAT	42.89	43.74	8.24-9.72	1.48
rMXPAT	41.15	44.31	8.24-11.19	2.95

uMXPAT	39.18	39.69	8.31-12.4	4.09
MXPATPNPA	38.53	44.08	8.2-11.98	3.78
MXPATPTh	40.29	42.99	8.42-12.36	3.94
MXPATPA	40.94	45.18	9.31-12.4	3.09
MXPATPPy	39.83	41.31	10.06-12.4	2.34
MXPATPN	37.82	39.33	8.2-12.4	4.2

Table S11. EMI shielding comparison of previous work published

	Composition	Polymer matrix	Fillers (%)	Density ($g.cm^{-3}$)	t (mm)	SE (dB)	SSE ($dB.g^{-1}.cm^3$)	SSE/t($dB.g^{-1}.cm^3$)	Ref.
1	$Ti_3C_2T_x$ /SA	SA	90	2.31	0.0008	57	24.6	30830	1
2	$Ti_3C_2T_x$ /CNF	Cellulose	90	2.10	0.047	25.8	12.44	2647	2
3	$Ti_3C_2T_x$ areogel	Bulk	MXene	0.0055	1	44.8	8145.5	81455.0	3
4	Ti_3CNT_x	Bulk	MXene	0.0055	1	42.3	7690.9	62909.0	3
5	Ti_2CT_x	Bulk	MXene	0.0055	1	48.5	8818.2	88182.0	3
6	CNT sponge	Bulk	CNT	0.018	2.4	20	1100.0	462.2	4
7	MWCNT/WPU Composites	WPU	MWCNT	0.02	2.3	23	1148.0	4991.0	5
8	CNF/Fe3O4	Epoxy	10	*	13	20	*	*	6
9	rGO/cellulose fiber	Cellulose	50	0.0028	5.0	47.8	16890.0	33780.0	7
10	CNT/polycarbonate	polycarbonate	20	1.13	2.1	39	34.5	154.0	8
11	high structure carbon black (HS-CB)/ABS	ABS	15	0.96	1.1	20	20.9	190	9
12	Graphene/ polyurethane (PU)	PU	GN	0.030	60	32	1066.7	177.8	10
13	SWCNT-Polystyrene foam	PS	7	0.56	1.2	18.5	33	275	11
14	carbon black filled EPDM	EPDM	37.5	0.594	2	18	30.3	15.1	12
15	Polypropylene/Stainless-Steel	PP	1.1	0.64	3.1	48	75	241.9	13
16	Polyetherimide/Graphene	PEI	10	0.291	2.3	12.8	44	191.3	14
17	C/MWCNTs/ Fe3O4	Phenolic foam	7	0.126	5	62	549	1098.7	15
18	Au/GN/Fe3O4/poly(dimethyl siloxane) (PDMS)	PDMS	*	0.116	2	30.5	263	1315	16
19	Polyimide/ reduced graphene	PI	16	0.022	0.8	21	937	11712	17

20	Greaphene foam	Bulk	GN	0.06	0.3	25.2	420	14000	18
21	Graphene/PDMS	PDMS	*	0.06	1	30	500	5000	18
22	Graphene-Polystyrene	PS	*	0.27	2.5	17.3	64.07	256.29	18
23	MXCS	CF	*	0.153	0.386	50.5	324.15	8397.78	19
24	MXCB	CF	*	0.229	0.398	47.6	205.52	5163.75	19
25	MWCNT/CNF	CNF	*	0.058	0.138	28.22	486.54	35256	19
26	Copper	Bulk	Bulk	9	3.1	90	10	32	20
27	Polypropylrnr/carbon fiber	PP	10 vol%	0.735	3.1	25	34	109	20
28	Stainless steel	Bulk	Bulk	8.091	4	89	11	27	20
29	Poly(ether sulfonate) (PES)-Nickel filaments	PES	7 vol %	1.851	2.85	87	47	165	20
30	PS-Cu nanowire	PS	2.1Vol %	*	0.21	35	*	*	20
31	MWCNT/ polyurethane	PU	10.6	*	0.4	24.7	*	*	21
32	Ag/PAN	PAN	20	*	0.75	40	*	*	22
33	Ag/BaTiO3	PVDF	20	*	1.2	21			22
34	Au/MWCNT	PVDF	3	*	0.5	26.7	*	*	22
35	GNP/PLLA	PLLA	15	*	1.5	15.5	*	*	22
36	MWCNT+PP	PP	8	*	3.2	29.47	*	*	23
37	CF+PP	PP	18	*	3.2	19.8	*	*	23
38	1 wt% CNT+30 wt% CF+PP	PP	31	*	1	16	*	*	23
39	SWCNTs/Epoxy	Epoxy	15	*	2	25	*	*	24
40	Graphite/PE	PE	18.7 vol%	*	3	33	*	*	24
41	MXPATPN	PAT-PpAP	*	1.217	0.62	45.18	33.26	236.45	This work
42	MXPATPNPA	PAT-PpAP-PANI	*	1.281	0.8	44.08	31.98	399.75	
	* indicates that the values were either not available or impossible to calculate.								

Table S12. The short-listed EMI shielding comparison for graph (Figure 11f)

Composition	No		Polymer matrix	t (mm)	SE (dB)
Ti3C2Tx /SA	1	MX/SA	SA	8.00E-04	57
Ti3C2Tx /CNF	2	MX/CNF	Cellulose	0.047	25.8
Ti3C2Tx areogel	3	MX/gel	Bulk	1	44.8
Ti3CNTx	4	MXN	Bulk	1	42.3

Ti2CTx	5	Ti2C	Bulk	1	48.5
CNT sponge	6	CNT/spo	Bulk	2.4	20
MWCNT/WPU Composites	7	CNT/PU/C	WPU	2.3	23
CNT/polycarbonate	8	CNT/PC	polycarbonate	2.1	39
high structure carbon black (HS-CB)/ABS	9	HSBC/ABS	ABS	1.1	20
SWCNT-Polystyrene foam	10	CNT/PS/foam	PS	1.2	18.5
carbon black filled EPDM	11	CB/EPDM	EPDM	2	18
Polypropylene/Stainless-Steel	12	PP/SS	PP	3.1	48
Polyetherimide/Graphene	13	PI/GN	PEI	2.3	12.8
Au/GN/Fe3O4/poly(dimethyl siloxane) (PDMS)	14	Au/GN/FeO	PDMS	2	30.5
Polyimide/ reduced graphene	15	PI/rGN	PI	0.8	21
Graphene foam	16	GN/foam	Bulk	0.3	25.2
Graphene/PDMS	17	GN/PDMS	PDMS	1	30
Graphene-Polystyrene	18	GN/PS	PS	2.5	17.3
MXCS	19	MXCS	CF	0.386	50.5
MXCB	20	MXCB	CF	0.398	47.6
MWCNT/CNF	21	CNT/CNF	CNF	0.138	28.22
Polypropylene/carbon fiber	22	PP/CF	PP	3.1	25
PS-Cu nanowire	23	PS/CuNW	PS	0.21	35
MWCNT/ polyurethane	24	CNT/PU	PU	0.4	24.7
Ag/PAN	25	Ag/PAN	PAN	0.75	40
Ag/BaTiO3	26	Ag/BTO	PVDF	1.2	21
Au/MWCNT	27	Au/CNT	PVDF	0.5	26.7
GNP/PLLA	28	GNP/PLLA	PLLA	1.5	15.5
MWCNT+PP	29	CNT/PP	PP	3.2	29.47
CF+PP	30	CF/PP	PP	3.2	19.8
1 wt% CNT+30 wt% CF+PP	31	CNT/CF/PP	PP	1	16
SWCNTs/Epoxy	32	CNT/epox	Epoxy	2	25
Graphite/PE	33	G/PE	PE	3	33
MXene-PAT-PpAP	34	MXPATPA	PAT-PpAP	0.62	45.18
MXene-PAT-PpAP-PANI	35	MXPATPNPA	PAT-PpAP-PANI	0.8	44.08

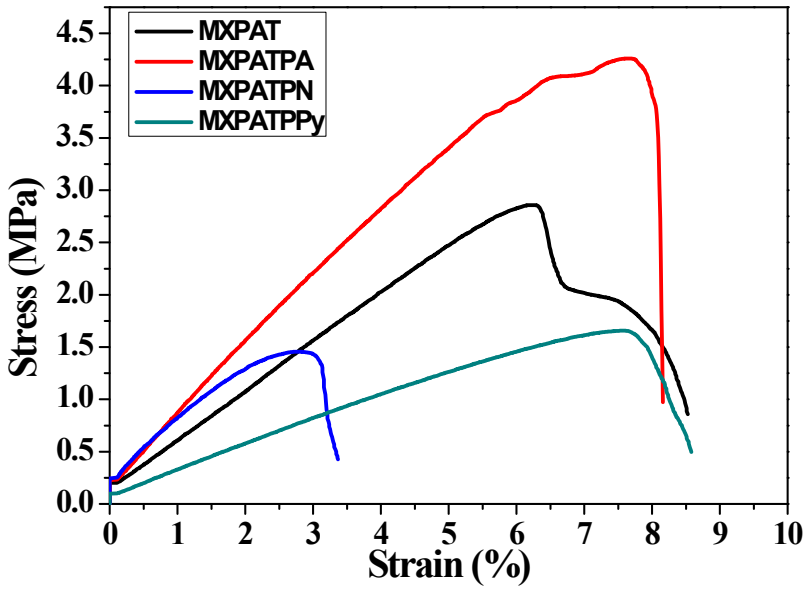

Figure S9. Stress and strain curve for composites

Reference.

1. Shahzad, F., Alhabeb, M., Hatter, C.B., Anasori, B., Hong, S.M., Koo, C.M. and Gogotsi, Y., 2016. Electromagnetic interference shielding with 2D transition metal carbides (MXenes). Science, 353(6304), pp.1137-1140.

2. Cao, W.T., Chen, F.F., Zhu, Y.J., Zhang, Y.G., Jiang, Y.Y., Ma, M.G. and Chen, F., 2018. Binary strengthening and toughening of MXene/cellulose nanofiber composite paper with nacre-inspired structure and superior electromagnetic interference shielding properties. ACS nano, 12(5), pp.4583-4593.

3. Han, M., Yin, X., Hantanasirisakul, K., Li, X., Iqbal, A., Hatter, C.B., Anasori, B., Koo, C.M., Torita, T., Soda, Y. and Zhang, L., 2019. Anisotropic MXene Aerogels with a Mechanically Tunable Ratio of Electromagnetic Wave Reflection to Absorption. Advanced Optical Materials, 7(10), p.1900267.

4. Crespo, M., González, M., Elías, A.L., Pulickal Rajukumar, L., Baselga, J., Terrones, M. and Pozuelo, J., 2014. Ultra-light carbon nanotube sponge as an efficient electromagnetic shielding material in the GHz range. physica status solidi (RRL)–Rapid Research Letters, 8(8), pp.698-704.

5. Zeng, Z., Jin, H., Chen, M., Li, W., Zhou, L. and Zhang, Z., 2016. Lightweight and anisotropic porous MWCNT/WPU composites for ultrahigh performance electromagnetic interference shielding. Advanced Functional Materials, 26(2), pp.303-310.

6. Crespo, M., Méndez, N., González, M., Baselga, J. and Pozuelo, J., 2014. Synergistic effect of magnetite nanoparticles and carbon nanofibres in electromagnetic absorbing composites. Carbon, 74, pp.63-72.

7. Wan, Y.J., Zhu, P.L., Yu, S.H., Sun, R., Wong, C.P. and Liao, W.H., 2017. Ultralight, super-elastic and volume-preserving cellulose fiber/graphene aerogel for high-performance electromagnetic interference shielding. Carbon, 115, pp.629-639.

8. Pande, S., Chaudhary, A., Patel, D., Singh, B.P. and Mathur, R.B., 2014. Mechanical and electrical properties of multiwall carbon nanotube/polycarbonate composites for electrostatic discharge and electromagnetic interference shielding applications. Rsc Advances, 4(27), pp.13839-13849.

9. Al-Saleh, M.H., Saadeh, W.H. and Sundararaj, U., 2013. EMI shielding effectiveness of carbon based nanostructured polymeric materials: a comparative study. Carbon, 60, pp.146-156.

10. Shen, B., Li, Y., Zhai, W. and Zheng, W., 2016. Compressible graphene-coated polymer foams with ultralow density for adjustable electromagnetic interference (EMI) shielding. ACS applied materials & interfaces, 8(12), pp.8050-8057.

11. Yang, Y., Gupta, M.C., Dudley, K.L. and Lawrence, R.W., 2005. Novel carbon nanotube− polystyrene foam composites for electromagnetic interference shielding. Nano letters, 5(11), pp.2131-2134.

12. Ghosh, P. and Chakrabarti, A., 2000. Conducting carbon black filled EPDM vulcanizates: assessment of dependence of physical and mechanical properties and conducting character on variation of filler loading. European Polymer Journal, 36(5), pp.1043-1054.

13. Ameli, A., Nofar, M., Wang, S. and Park, C.B., 2014. Lightweight polypropylene/stainless-steel fiber composite foams with low percolation for efficient electromagnetic interference shielding. ACS applied materials & interfaces, 6(14), pp.11091-11100.

14. Ling, J., Zhai, W., Feng, W., Shen, B., Zhang, J. and Zheng, W.G., 2013. Facile preparation of lightweight microcellular polyetherimide/graphene composite foams for electromagnetic interference shielding. ACS applied materials & interfaces, 5(7), pp.2677-2684.

15. Li, Q., Chen, L., Ding, J., Zhang, J., Li, X., Zheng, K., Zhang, X. and Tian, X., 2016. Open-cell phenolic carbon foam and electromagnetic interference shielding properties. Carbon, 104, pp.90-105.

16. Sun, Y., Luo, S., Sun, H., Zeng, W., Ling, C., Chen, D., Chan, V. and Liao, K., 2018. Engineering closed-cell structure in lightweight and flexible carbon foam composite for high-efficient electromagnetic interference shielding. Carbon, 136, pp.299-308.

17. Li, Y., Pei, X., Shen, B., Zhai, W., Zhang, L. and Zheng, W., 2015. Polyimide/graphene composite foam sheets with ultrahigh thermostability for electromagnetic interference shielding. RSC Adv 5 (31): 24342–24351. J Mater Chem C, 3(26), pp.6589-6599.

18. Shen, B., Li, Y., Yi, D., Zhai, W., Wei, X. and Zheng, W., 2016. Microcellular graphene foam for improved broadband electromagnetic interference shielding. Carbon, 102, pp.154-160.

19. Raagulan, K., Braveenth, R., Ro Lee, L., Lee, J., Kim, B.M., Moon, J.J., Lee, S.B. and Chai, K.Y., 2019. Fabrication of Flexible, Lightweight, Magnetic Mushroom Gills and Coral-Like MXene–Carbon Nanotube Nanocomposites for EMI Shielding Application. Nanomaterials, 9(4), p.519.

20. Ameli, A., Nofar, M., Wang, S. and Park, C.B., 2014. Lightweight polypropylene/stainless-steel fiber composite foams with low percolation for efficient electromagnetic interference shielding. ACS applied materials & interfaces, 6(14), pp.11091-11100.

21. Li, H., Yuan, D., Li, P. and He, C., 2019. High conductive and mechanical robust carbon nanotubes/waterborne polyurethane composite films for efficient electromagnetic interference shielding. Composites Part A: Applied Science and Manufacturing, 121, pp.411-417.

22. Li, J., Peng, W.J., Fu, Z.J., Tang, X.H., Wu, H., Guo, S. and Wang, M., 2019. Achieving high electrical conductivity and excellent electromagnetic interference shielding in poly (lactic acid)/silver nanocomposites by constructing large-area silver nanoplates in polymer matrix. Composites Part B: Engineering, 171, pp.204-213.

23. Shajari, S., Arjmand, M., Pawar, S.P., Sundararaj, U. and Sudak, L.J., 2019. Synergistic effect of hybrid stainless steel fiber and carbon nanotube on mechanical properties and electromagnetic interference shielding of polypropylene nanocomposites. Composites Part B: Engineering, 165, pp.662-670.

24. Wang, L., Qiu, H., Liang, C., Song, P., Han, Y., Han, Y., Gu, J., Kong, J., Pan, D. and Guo, Z., 2019. Electromagnetic interference shielding MWCNT-Fe3O4@ Ag/epoxy nanocomposites with satisfactory thermal conductivity and high thermal stability. Carbon, 141, pp.506-514.